

MACHINABILITY OF HIGH Mn STEEL USING TOOL LIFE CRITERIA

Dika Handayani and Victor F. Okhuysen

Industrial and Manufacturing Engineering Department, California State Polytechnic University, 3801 West Temple Avenue, Pomona, CA 91768, USA

Nicole Wagner

Dale E. and Sarah Ann Fowler School of Engineering, Chapman University, One University Drive, Orange, CA 92866, USA

Copyright © 2023 The Author(s)
<https://doi.org/10.1007/s40962-023-01044-3>

Abstract

High Mn steel alloys have shown to provide both high strength and ductility. However, current literature offers limited guidance on the machinability of these steel alloys. Therefore, this work provides turning recommendations for high Mn steel that is based on tool life data. Several indexable carbide inserts with various rake angles were used to machine cast billets of high Mn steel. Turning characteristics from various feed rates, cutting speeds, and depths of cut were analyzed. Through a design of experiments, it was determined that the feed rate was the most significant factor affecting tool life and that a tool with a negative rake angle had a longer tool life than one with a positive rake angle. The effect of coolant on tool life was seen to be dependent on the tool material. Optimal cutting conditions, which provided a long tool life while maintaining a decent material removal rate, were found for a

cutting speed of 150 ft/min, a feed rate of 0.008 in/rev, and a depth of cut of 0.080 inches. In addition, microhardness analysis was used to determine the thickness of the work-hardened layer on machined surfaces. Microhardness was seen to increase between 0.028 and 0.040 inches from the machined surfaces for each cutting condition, explaining the difficulty experienced in machining high Mn steel alloys. The availability of these recommendations for machining high Mn steel encourages the application of this material in a more efficient and productive manner.

Keywords: high Mn steel, machining, turning, tool life, microhardness

Introduction

The use of high Mn steel as lightweight structural alloy has been increasingly important. However, high Mn steel has low machinability because of its low thermal conductivity. In addition, high Mn steels tend to work harden through the transformation of austenite to martensite at the high plastic strains observed during machining.¹⁻³ The lack of fundamental machining guidelines has limited full application of this material, especially since machining operations are essential for a casting to meet final dimensional and tolerance requirements. Few studies have investigated machining high Mn steels, yielding low tool life even at

low cutting speeds. In their turning experiments, Grams and Bartlett¹ found that machining high Mn steel in the solution treated condition using a deeper cut resulted in less tool wear. The highest tool life of less than 10 min was obtained when machining the aged condition with a cutting speed of 30 ft/min, a feed rate of 0.008 in/rev, and a depth of cut of 0.04 inches.

Tuttle² compared the machinability of high Mn-C (306 BHN) with ASTM A723 Grade 2 steel in the quenched and tempered state (378 BHN) at the same cutting speed (100 ft/min) using milling and drilling processes. The end mill used in this study to machine the high Mn steel shattered before completing the plate, while the tool used with the ASTM A723 Grade 2 steel machined the plate with no issue. In their drilling experiments, tools showed severe wear while machining high Mn steel. The low

Table 1. Average Chemical Composition of Workpieces

Fe	Mn	Al	Si	C	Mo	Cu	Cr	V	Ni	S	P	Sn
60.61	28.83	8.14	1.04	0.852	0.456	0.026	0.017	0.015	0.006	0.006	0.004	<0.001

machinability of high Mn alloy steel is attributed to the high work hardening rate caused by the mechanical twins during the machining process.

Smaga et al.³ investigated the micromachined surface of X30MnAl17-1 steel. In this study, traces of hcp-martensite were observed on the micro-ground and micro-milled surfaces. Similar machining challenges have been reported for other materials with limited austenite stability. Due to the limited literature on the machining of high Mn or TWIP steels, other austenite-containing steels with a tendency to work harden have been examined. Studies on Hadfield and austenitic stainless steels have been used as a basis to provide machining recommendations for high Mn steel. The poor machinability of Hadfield steel is caused by its strain hardening behavior. Sant and Smith⁴ explained that defects, such as twinning and stacking faults, start forming at the intermediate strains and continue to interact at high strains observed on machined surfaces. The formation of these defects initiates the strain-induced hcp ϵ -martensitic transformation in Hadfield steels. Horng et al.⁵ evaluated flank wear and surface roughness to provide recommendations for machining Hadfield steels in hard turning with ceramic tools. In a dry turning study on Hadfield steels, Kuljanic et al.⁶ described relevant work hardening of Hadfield steels after the machining process, citing severe wear on both the primary and secondary flank faces, and the rake face. A TiCN+Al₂O₃-coated carbide insert with chamfered cutting edge and positive effective rake angle was recommended to obtain optimum tool life. Havel⁷ recommended using a tool with a negative rake angle, along with low surface speed and large depth of cut.

Some studies have focused on using high Mn Hadfield steels as a replacement for austempered ductile iron (ADI).⁸ The work conducted by Skoczylas et al.⁹ resulted in comparable wear resistance for these materials. Another study done by Bhero¹⁰ concluded that the ADI surface was tougher, while that of the Hadfield steel was harder and more brittle.

Another class of steels that have low machinability include austenitic stainless steels. While these steels are widely used for their high tensile strength and high ductility, these factors increase the tendency to form a built-up edge (BUE) during machining.¹¹ In addition, the low thermal conductivity and gumminess of austenitic stainless steel increases the likelihood of forming a BUE.¹² To minimize or avoid BUE formation, an appropriate cutting speed

should be selected. Increased cutting speeds up to 200 m/min (656 ft/min) have shown to increase tool life.¹³ Furthermore, the use of a low feed rate must be avoided to minimize the work-hardening effect.¹² Deep cuts are also recommended when machining austenitic stainless steel.^{14,15} In addition, a cutting tool with a rake angle between 5 and 20° and greater side clearance angles is suggested to reduce rubbing and surface work hardening during turning.¹¹

The focus of this study was to provide recommendations for turning high Mn steel. Cutting tools based on TiN and AlCr₂O₃ were used in both dry and wet machining conditions. A modified Taylor tool life equation was generated to predict the tool life given a selected set of turning parameters. In addition, microhardness analysis was conducted to ascertain the thickness of the work-hardened layer. Tool wear and material removal rate were determined for various machining parameters, to provide recommendations of cutting speed, feed rate, and depth of cut for high Mn steels.

Experimental Procedure

Materials and Equipment

In this study, a series of turning experiments were conducted to assess the machinability of high Mn steel using tool life as the criteria. These tool life experiments focused on varying the machining parameters (cutting speed, feed rate, and depth of cut) as well as the cutting tool/geometry and the use of coolant. The effects of cutting speeds on the tool life were then analyzed to provide starting recommendations for turning high Mn steel.

The workpieces used in this study were produced in a commercial foundry by investment casting in the form of 4-inch-diameter cylinders with 12 inch length by Spokane Industries. The chemical composition of these cylinders is shown in Table 1. The workpieces had a standard solution treatment at 1050 °C for 4 h and were water quenched, producing a Brinell hardness of 176 ± 4 BHN. In addition, X-ray analysis was done to ensure there was no centerline shrinkage in the cylinders.

Turning experiments (Figure 1) were performed on a Haas TL-1 CNC lathe. Before each experiment, the outer surface of the cylinder was trued using a manual lathe to establish

the datum. In addition, a center was machined into one end of the cylinder for tailstock support during the experiments. The workpiece was secured between a 3-jaw chuck and the tailstock. To maintain a consistent surface between workpieces, any remaining scale from casting was removed prior to each experiment. Each cylinder was machined to include multiple passes. After each pass, the wear on the cutting tool was measured and 0.25 inches of each pass was preserved for microhardness testing. Test runs were randomized.

In this study, three different indexable carbide inserts from Sandvik Coromant were used with a DCLNR 12 4B tool holder. Table 2 provides the classification, coating material, and geometry for each insert. The MM 1115 (ISO-M) and SF 1115 (ISO-M) have a more positive rake angle than the PM 4315 (ISO-H). Inserts MM 1115 and SF 1115 were recommended by the manufacturer for machining austenitic stainless steel, while PM 4315 was intended for hardened steel. The primary difference between MM 1115 and SF 1115 is the rake angle; the SF 1115 insert has a more positive rake angle than MM 1115.

Procedure

Turning tool life experiments were conducted according to ISO 3685: Tool-life testing with single-point turning tools.¹⁶ According to this standard, useful tool life is defined as the time when the inserts reached a maximum flank wear penetration, or VB_{max} , and is measured either as



Figure 1. Turning experiment setup.

uniform wear of 0.01 inches (0.3 mm) or localized wear of 0.02 inches (0.6 mm). In this study, localized wear measurements were made after each pass using a Nikon SMZ800N stereoscope.

The selection of cutting parameters, tool materials and geometry is believed to influence the amount of work-hardened layer formation when machining high Mn. This tendency of high Mn to work harden contributes to its poor machinability. Therefore, low and high values of feed rates and depths of cut were set to be 0.008–0.015 in/rev and 0.030–0.060 inches, respectively. These initial settings were selected based on the recommendations from the tool manufacturer and guidelines found in ISO 3685.¹⁶ In addition, Sandvik Coromant recommends using a feed rate between 0.008 and 0.018 in/rev and a depth of cut of 0.100 inches. These values are in line with the ISO 3685 guidelines of a starting feed rate and depth of cut of 0.010 in/rev and 0.100 inches, respectively, for 1/32 inch corner radius. The minimum depth of cut is limited to be twice the corner radius or 0.060 inches (per ISO 3685), and the minimum feed rate is set to be 0.008 in/rev (per Sandvik Coromant). The cutting speeds were selected to match the 10hp power capacity of the lathe used in this study. Since the specific cutting horsepower of this high Mn steel was unknown, a conservative range of cutting speeds (80–160 ft/min) was selected.

As there is no agreement in the literature on whether the coolant provides positive effect on tool life when machining work hardened materials, this study also aimed to analyze the effect of coolant on tool life. The coolant used in this study was ValCool with 5–7% concentration.

Design of Experiments

Screening Experiments

A Plackett-Burman fractional factorial experiment with eight runs and two replications was used for screening to economically detect large main effects. The five factors

Table 2. Cutting Tool Inserts

CNMG 432 MM 1115 PVD TiAlN + AlCr ₂ O ₃	CNMG 432 SF 1115 PVD TiAlN + AlCr ₂ O ₃	CNMG 432 PM 4315 CVD TiCN + AlCr ₂ O ₃ + TiN

used were feed rate, depth of cut, cutting speed, tool material and geometry, and coolant usage. Two levels were used as the maximum and minimum. Table 3 shows a summary of the factors, which were selected in consideration of a literature review^{1,2, 13–16} for turning experiments using carbide tool and the trial runs. Insert MM 1115 was used as the low setting in the first replication, while insert SF was used in the second replication of the low setting of tool material and geometry. The run sets for the screening experiments are summarized in Table 4. Randomization was done to minimize any potential biases in the experiment.

Main Experiments

The screening experiment revealed that the feed rate of 0.008 in/rev with the combination of the MM 1115 insert and use of coolant resulted in a longer tool life. Therefore, in the main experiment, feed rate, tool material and geometry, and coolant were held constant, while only cutting speed and depth of cut were varied. A testing range of 150–250 ft/min for cutting speed and 0.010–0.080 inches for depth of cut were considered. Figure 2 indicates the test values used in the main experiment with an X. To

Table 3. Design Scheme Of Machining Parameters for Screening Experiments

Factors	(–1) Level	(+1) Level
A Feed rate (in/rev)	0.008	0.015
B Depth of cut (in)	0.030	0.060
C Cutting speed (ft/min)	80	160
D Tool material/geometry	REP #1: MM 1115 REP #2: SF 1115	PM 4315
E Coolant	Dry	Flood

Table 4. Design Layout of Screening Experiments

Run	A Feed rate	B Depth of cut	C Speed	D = ABC Tool material/geometry	E = BC Coolant
1	–1	–1	–1	–1	+1
2	–1	–1	+1	+1	–1
3	–1	+1	–1	+1	–1
4	–1	+1	+1	–1	+1
5	+1	–1	–1	+1	+1
6	+1	–1	+1	–1	–1
7	+1	+1	–1	–1	–1
8	+1	+1	+1	+1	+1

ensure that the range selected was not too conservative, the experiment started with the most aggressive combination (250 ft/min cutting speed and 0.080 inch depth of cut). If the tool lasted more than 10 min, then the next experiment was to increase the cutting speed and/or the depth of cut. However, since a short tool life was obtained with the combination of 250 ft/min cutting speed and 0.080 inch depth of cut, the subsequent approach was to decrease one and increase the other parameter (i.e., moving diagonally in the matrix in Figure 2). Once these runs were completed, the tests were continued to area inside the 150–250 ft/min cutting speed and 0.010 to 0.080 inch depth of cut boundary. Two replications were conducted to assess tool life using the same cutting parameters, and randomization was done to minimize biases.

Work-Hardened Layer

A Tinius Olsen FH-14 microhardness tester was used to verify the presence of a work-hardened layer after machining and determine the thickness of this layer, if present. Samples for microhardness testing were prepared by sectioning portions from the machined cylinders by wire EDM and polished to a one micrometer (4×10^{-5} inches) roughness. Vickers microhardness was measured on the machined surfaces in both the radial and tangential direction. As seen in Figure 3, the radial direction was the depth of cut and the tangential direction was the feed rate. For

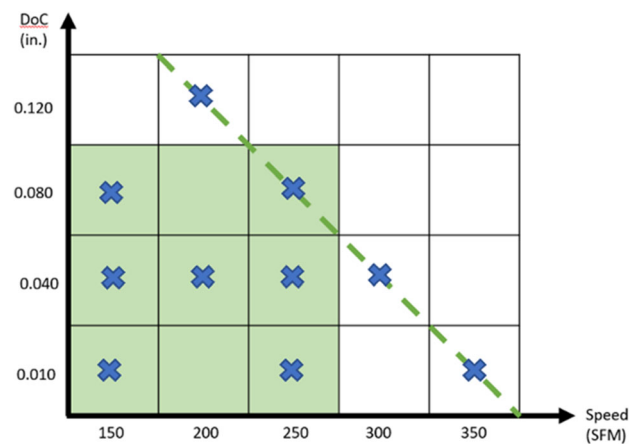


Figure 2. Design matrix for the main experiment.

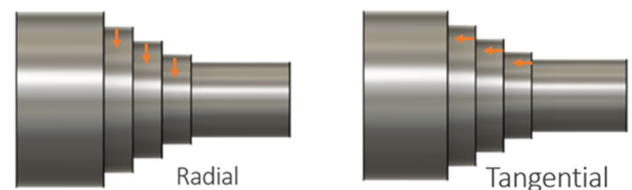


Figure 3. Radial and tangential directions to machined surface.

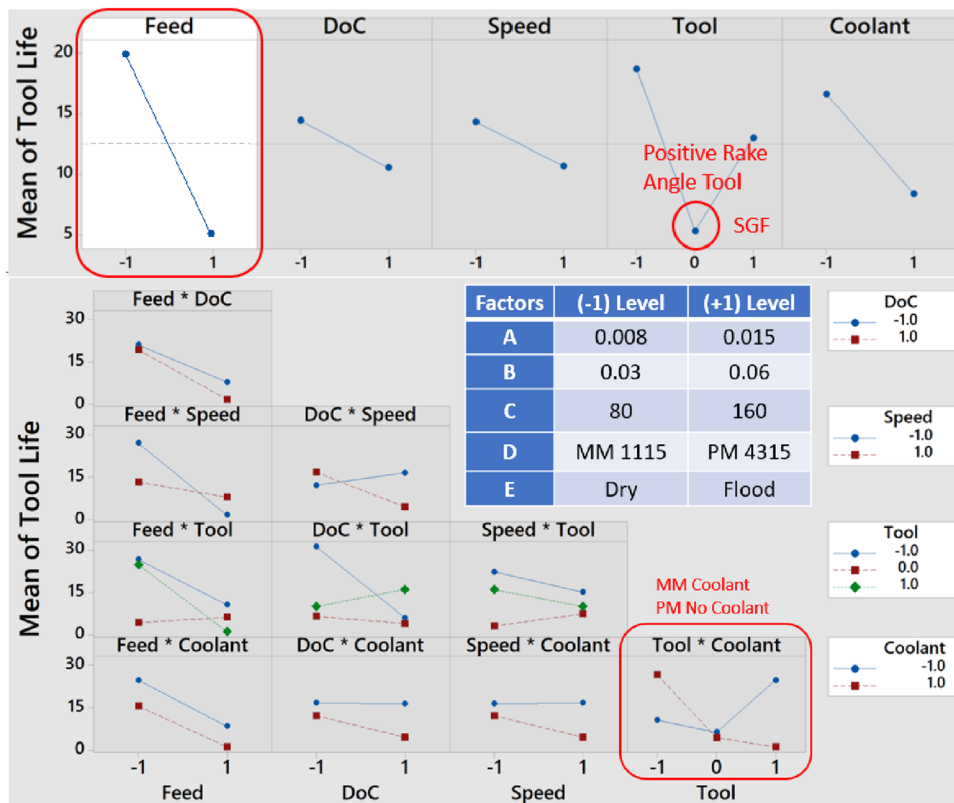


Figure 4. Summary of effects determined from screening experiment.

each microhardness measurement, a 100-g load was applied for a dwell time of 15 s, in accordance with the ASTM Test Method for Microindentation Hardness of Materials—E384.¹⁷

Results and Discussion

To determine whether the cutting parameters to be used in the screening experiments were appropriate, a few pilot experiments were conducted. From these results, it was determined that the intended settings of depth of cut of 0.160 inches was too aggressive, and thus, it was adjusted to 0.060 inches maximum for the screening experiment from the original intent of 0.080 and 0.160 inches.

Screening Experiment

Figure 4 shows a summary of the effects found in the screening experiment. It was observed that the 0.015 in/rev feed rate lowered tool life excessively, and therefore, the 0.008 in/rev was used for the main experiment. In addition, the results showed that a tool with a negative rake angle had a higher tool life than that with a positive rake angle. This is expected as a negative rake provides a stronger tool tip than a positive rake, making the tool with a negative rake more resilient under impact loading conditions. Finally, the screening experiment revealed that the MM

insert with coolant had a longer tool life than the PM insert without coolant. Therefore, the MM tool insert was chosen for use in the main experiment. Furthermore, in the main experiment, feed rate, tool material and geometry, and coolant were held constant, while tool life was determined for the factors of cutting speed and depth of cut.

Main Experiment

During the main experiment, feed rate was held constant at 0.008 in/rev. The lower feed rate of 0.008 in/rev was selected since it showed a significantly higher tool life than the higher feed rate of 0.015 in/rev. In addition, the MM insert was used with coolant in the main experiment. This tool was selected for the main experiment because it is the stainless steel designated tool with a physical vapor deposition (PVD) coating of TiAlN + AlCr₂O₃ and negative rake angle. As seen in Figure 5, the coating on the MM insert maintained a higher hardness at higher temperatures. The aluminum oxide layer that was formed between the chip and the tool during machining removed heat more effectively.

Using the MM insert, three levels were used for the cutting speed and depth of cut, resulting in the 3 × 3 fractional factorial matrix (highlighted area in Figure 2). The initial intent was to execute a design with the four corners and center value only. However, as the results were received it

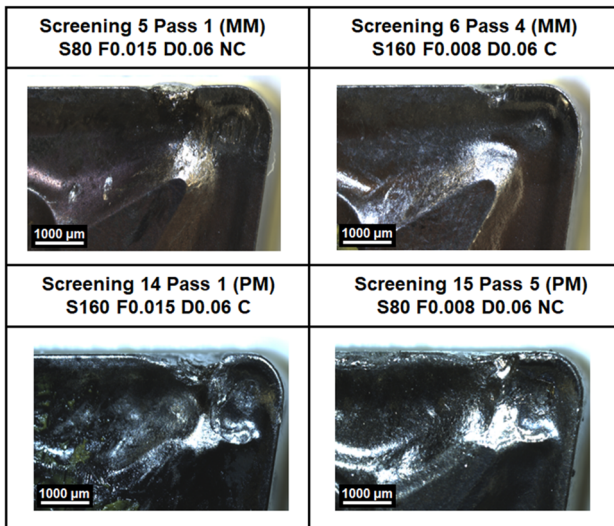


Figure 5. Crater wear of MM and PM inserts.

was perceived as beneficial to obtain more data and the additional runs were performed to test the limits of machinability as well as gather more data at the 0.040 inch depth of cut. To ensure that the selection was not too conservative, initial experiments were conducted using conditions at the top right corner of the matrix, with additional experiments run along the diagonal shown in Figure 2 and in some of the empty spots of the fractional factorial design.

Turning tool life experiments were conducted according to the ISO 3685 standard on tool-life testing with single-point turning tools.¹⁶ According to this standard, tool life is regarded as the time when tool inserts reach a maximum flank wear penetration, or VB_{max} . The localized wear of VB_{max} was measured using a Nikon SMZ800N stereoscope. In this study, the threshold of the tool wear criterion VB_{max} was 0.02 inches at 10 min. Parameters for which tool inserts reached the VB_{max} threshold prior to 10 min were discarded.

Figure 6 shows tool life determined by amount of material removed (MR) at the point the VB_{max} threshold was reached, as a function of cutting speed and depth of cut. This is consistent with what is known that as cutting speed increases, tool life greatly decreases. In addition, for work-hardened materials, the depth of cut needs to go deeper than the work-hardened layer. It is seen that a combination of moderate cutting speed of 150 ft/min and a depth of cut of 0.08 inches produced the highest total material removed.

In Figure 7, cutting speed (S) and depth of cut (D) are combined in the material removal rate (MRR). Tool life is again represented by the total material removed (MR). It is seen that the cutting parameters that produced the longest tool life, while maintaining a high material removal rate is for a cutting speed of 150 ft/min and a depth of cut of 0.08

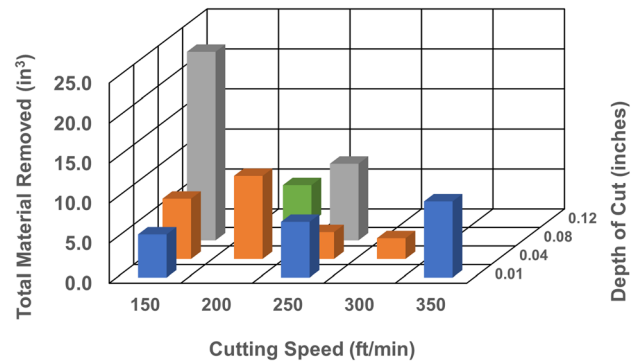


Figure 6. Total material removed at $VB_{max} = 0.6$ mm for different cutting speeds and depths of cut.

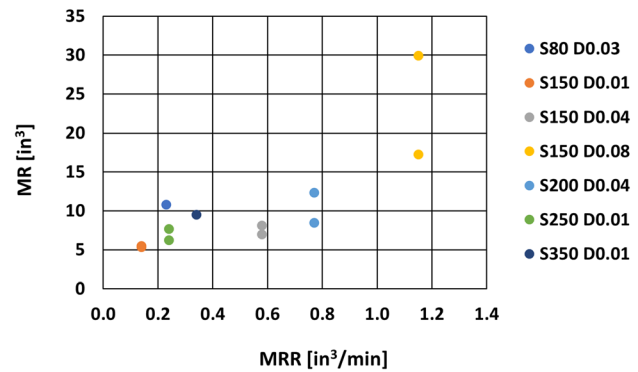


Figure 7. Total material removed as a function of material removal rate.

inches. Using these parameters, along with the feed rate of 0.008 in/rev that was held constant for all experiments, a modified Taylor tool life equation was generated.

The Taylor tool life equation¹⁸ states that

$$VT^n = C \quad \text{Eqn. 1}$$

where V is the cutting speed in ft/min and T is the desired tool life in minutes. In this equation, n and C are constants, whose values depend on cutting conditions, work and tool material properties, and tool geometry. The modified Taylor tool life includes variables for depth of cut, d , and feed rate, f , giving

$$VT^n d^x f^y = C \quad \text{Eqn. 2}$$

where n , x and y are constants to be determined experimentally. When the feed rate is set to 0.008 in/rev, the modified Taylor tool life equation for high Mn steel becomes

$$VT^{0.57} d^{0.55} f^y = C \quad \text{Eqn. 3}$$

This modified Taylor tool life equation can be used to determine the starting turning parameters needed to achieve a desired tool life or to predict the tool life given a set of turning parameters. It should be noted that parameters only

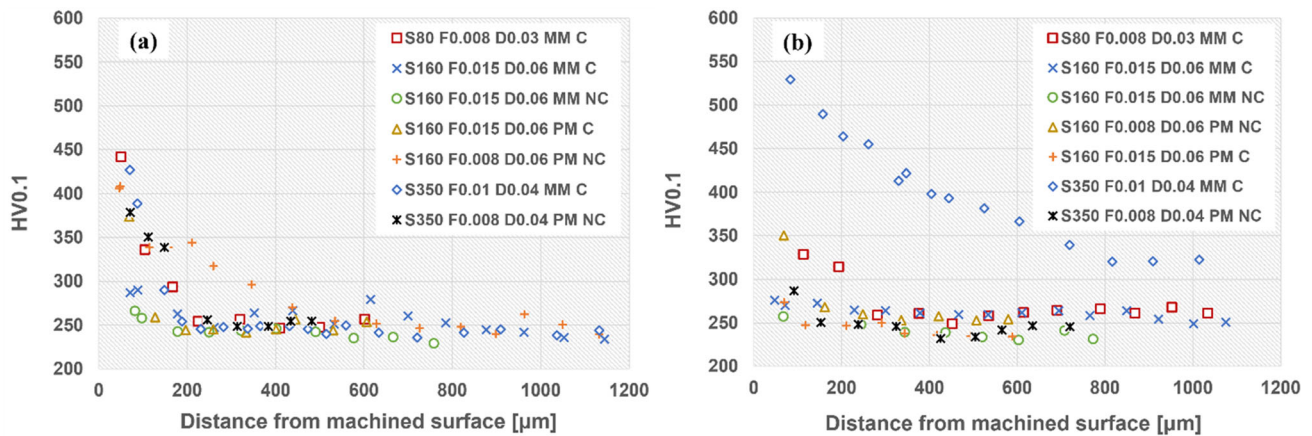


Figure 8. Microhardness measurements on machined surfaces on (a) radially and (b) tangential direction.

within the ranges used in this study are valid with this equation. A set of turning parameter of a feed rate of 0.008 in/rev, cutting speed of 150 ft/min, and a depth of cut of 0.08 inches resulted in the best combination of long tool life with higher total material removed.

Work-Hardened Layer

The low machinability of high Mn steel is attributed to its high work hardening rate. Therefore, the presence of a work-hardened layer was expected and confirmed on the machined surfaces using microhardness analysis. Further examination determined the thickness of the work-hardened layer and whether cutting parameters affected its thickness. Figure 8 shows microhardness measurements, using a 100-g load for Vickers microhardness (HV 0.1), on machined surfaces in both the (a) radially and (b) tangential orientation. A single area was selected for measurement on each specimen. Machining conditions, including cutting speed (S), feed rate (F), depth of cut (D), insert type, and either coolant or no coolant are indicated for each specimen. Close to the machined surface, microhardness values twice that of the interior, or bulk, were observed. From this rapid decline in microhardness, it is concluded that these elevated hardness values confirm the presence of the work-hardened layer. It is noted that bulk hardness was reached in a range between 200 and 700 μm (0.008–0.028 in) from the machined edge. This finding correlates to the recommendation to machine with a depth of cut deeper than 700 μm (0.028 in) to go beyond the work-hardened layer. One noteworthy anomaly was observed for microhardness values taken tangentially from the machined surface for a cutting speed of 350 ft/min, a feed rate of 0.010 in/rev and a depth of cut of 0.04 inches. The observed elevated microhardness was attributed to the combination of very high cutting speed and high feed rate.

Conclusion

High Mn steel alloys are desirable for use in applications that require both high strength and ductility. This study was inspired to expand the literature and offer guidance on machining these steel alloys. Tool wear and material removal rate were related to turning parameters that included feed rate, cutting speed, depth of cut, tool material and geometry, and use of coolant. Recommendations for machining high Mn steel include using a negative rake angle tool, such as an insert with a PVD coating of TiAlN and AlCr_2O_3 , for better resistance to crater wear. High tool life was found for turning parameters that included a feed rate of 0.008 in/rev, cutting speed of 150 ft/min, and a depth of cut of 0.08 inches. A modified Taylor tool life was generated to determine turning parameters for a desired tool life. In addition, a work-hardened layer was confirmed using microhardness measurements taken both radially and tangentially from the machined surface.

Acknowledgements

The authors would like to thank the DLA-Troop Support, Philadelphia, PA and the Defense Logistics Agency Information Operations, J68, Research & Development, Ft. Belvoir, VA, for sponsoring this research.

Funding

Open access funding provided by SCEL, Statewide California Electronic Library Consortium.

Conflict of interest The publication of this material does not constitute approval by the government of the findings or conclusion herein. Wide distribution or announcement of this material shall not be made without specific approval by the sponsoring government activity.

Open Access This article is licensed under a Creative Commons Attribution 4.0 International License, which permits use, sharing, adaptation, distribution and reproduction in any medium or format, as

long as you give appropriate credit to the original author(s) and the source, provide a link to the Creative Commons licence, and indicate if changes were made. The images or other third party material in this article are included in the article's Creative Commons licence, unless indicated otherwise in a credit line to the material. If material is not included in the article's Creative Commons licence and your intended use is not permitted by statutory regulation or exceeds the permitted use, you will need to obtain permission directly from the copyright holder. To view a copy of this licence, visit <http://creativecommons.org/licenses/by/4.0/>.

REFERENCES

1. M. Grams, L. Bartlett, Machinability and Notch Toughness of High Manganese and Aluminum Steels. In: 119th Metalcasting Congress (2015).
2. R. Tuttle, Preliminary Machinability Study of Fe-Mn-Al-C Steel. AFS Trans. **120**, 1–12 (2012)
3. M. Smaga, T. Beck, P. Arrabiyeh, I. Reichenbach, B. Kirsch, J.C. Aurich, Characterization of Micro Machined Surface from TRIP/TWIP Steels. In: MATEC Web Conferences **33**, 07004 (2015)
4. S.B. Sant, R.W. Smith, A study in the work-hardening behavior of austenitic manganese steels. J. Mater. Sci. **22**, 1808–1814 (1987)
5. J. Horng, N. Liu, K. Chiang, Investigating the machinability evaluation of Hadfield steel in the hard turning with Al₂O₃/TiC mixed ceramic tool based on the response surface methodology. J. Mater. Process. Technol. **208**, 532–541 (2008)
6. E. Kuljanic, M. Sortino, G. Totis, F. Prospero, Evaluation of Commercial Tools for Machining Special-Alloy Hadfield Steel. In: Proceedings from the IX International Congress on Machines, Technologies, Materials (2012).
7. D. Havel, Austenitic Manganese Steel: A Complete Overview. Steel Founders' Society of America Technical & Operating (2017).
8. A. Kochański, A. Krzyńska, T. Chmielewski, A. Stoliński, Comparison of austempered ductile iron and manganese steel wearability. Arch. Foundry Eng. **15**(1), 51–54 (2015)
9. P. Skoczylas, A. Krzyńska, M. Kaczorowski, The comparative studies of ADI versus Hadfield cast steel wear resistance. Arch. Foundry Eng. **11**(2), 123–126 (2011)
10. S. Bhero, Hadfield Steel and Austempered Ductile Iron: Similar in Metallurgy yet Different in Chemistry, Heat Treatment and Application. In: *International Conference on Mining, Minerals and Metallurgical Engineering* (2015), pp 49–52.
11. Carpenter Technology Corporation, Guide to Machining Carpenter Specialty Alloys. (CRS Holdings, Wyomissing, , pp 1–167) (2002).
12. M. Kaladhar, K.V. Subbaiah, C.H.S. Rao, Machining of austenitic stainless steels—a review. Int. J. Mach. Mach. Mater. **12**, 178–192 (2012)
13. C. Özek, A. Haşçalık, U. Çaydaş, F. Karaca, E. Ünal, Turning of AISI 304 Austenitic Stainless Steel. J. Eng. Nat. Sci. 117–121 (2006).
14. Sandmeyer Steel Company, “Alloy 303 Austenitic Stainless Steel Plate,” <https://www.sandmeyersteel.com/303.html>, visited on November 7, 2021.
15. British Stainless Steel Association, “General principles of machining stainless steels,” https://bssa.org.uk/bssa_articles/general-principles-of-machining-stainless-steels/, visited on November 7, 2021.
16. International Standard ISO 3685: “Tool-life testing with single-point turning tool.” (1993).
17. ASTM E384-17: “Standard Test Method for Microindentation Hardness of Materials.” (2017)
18. Kalpakjian, S. Manufacturing Engineering and Technology, 7th edition (Pearson, London) (2014).

Publisher's Note Springer Nature remains neutral with regard to jurisdictional claims in published maps and institutional affiliations.